

On the Robustness of Bayesian Neural Networks to Adversarial Attacks

L. Bortolussi, Ginevra Carbone, Luca Laurenti, Andrea Patane, Guido Sanguinetti, Matthew Wicker

arXiv:2207.06154v2 [cs.LG] 10 Jul 2023

Abstract—Vulnerability to adversarial attacks is one of the principal hurdles to the adoption of deep learning in safety-critical applications. Despite significant efforts, both practical and theoretical, training deep learning models robust to adversarial attacks is still an open problem. In this paper, we analyse the geometry of adversarial attacks in the over-parameterised limit for Bayesian Neural Networks (BNNs). We show that, in the limit, vulnerability to gradient-based attacks arises as a result of degeneracy in the data distribution, i.e., when the data lies on a lower-dimensional submanifold of the ambient space. As a direct consequence, we demonstrate that in this limit BNN posteriors are robust to gradient-based adversarial attacks. Crucially, by relying on the convergence of infinitely-wide BNNs to Gaussian Processes (GPs), we prove that the expected gradient of the loss with respect to the BNN posterior distribution is vanishing, even when each neural network sampled from the posterior is vulnerable to gradient-based attacks. Experimental results on the MNIST, Fashion MNIST, and half moons datasets with BNNs trained with Hamiltonian Monte Carlo and Variational Inference, support this line of arguments, empirically showing that BNNs can display both high accuracy on clean data and robustness to both gradient-based and gradient-free adversarial attacks.

Index Terms—Bayesian Neural Networks, Adversarial Attacks, Adversarial Robustness, Bayesian Inference

I. INTRODUCTION

Adversarial attacks are small, potentially imperceptible, perturbations of test inputs that can lead to catastrophic misclassifications in high-dimensional classifiers such as deep Neural Networks (NN). Since the seminal work of Szegedy et al. [1] adversarial attacks have been intensively studied and even highly accurate state-of-the-art deep learning models, trained on very large data sets, have been shown to be susceptible to such attacks [2, 3]. In the absence of effective defenses, the widespread existence of adversarial examples has raised serious concerns about the security and robustness of models learned from data [4]. As a consequence, the development of machine learning models that are robust to adversarial perturbations is an essential pre-condition for their application in safety-critical

Luca Bortolussi with the Department of Mathematics and Geosciences, University of Trieste, Trieste, Italy, and Modeling and Simulation Group, Saarland University, Saarland, Germany.

Ginevra Carbone with the Department of Mathematics and Geosciences, University of Trieste, Trieste, Italy.

Luca Laurenti is with Delft Center of Systems and Control, TU Delft University, The Netherlands.

Andrea Patane with the School of Computer Science and Statistics, Trinity College, Dublin, Ireland.

Guido Sanguinetti is with the School of Informatics, University of Edinburgh, Edinburgh, United Kingdom, and SISSA, International School of Advanced Studies, Trieste, Italy.

Matthew Wicker is with the Department of Computer Science, University of Oxford, Oxford, United Kingdom.

scenarios, such as autonomous driving, where model failures can lead to fatal or costly accidents.

Many adversarial attack strategies are based on identifying directions of high variability in the loss function by evaluating the gradient w.r.t. to the neural network input [2, 5]. Since such variability can be intuitively linked to uncertainty in the prediction, Bayesian Neural Networks (BNNs) [6, 7, 8, 9] have been recently suggested as a more robust deep learning paradigm, a claim that has also found empirical support [10, 11, 12, 13, 14]. However, neither the source of this robustness, nor its general applicability are well understood mathematically.

In this paper we show a remarkable property of BNNs: in a suitably defined limit, we prove that the gradients of the expected loss function of an infinitely-wide BNN w.r.t. the input vanish. Our analysis shows that adversarial attacks for highly accurate NNs arise from the low dimensional support of the data generating distribution. By averaging over nuisance dimensions, under certain assumptions on the data manifold geometry, BNNs achieve zero expected gradient of the loss and are thus, provably immune to gradient-based adversarial attacks. Specifically, we first show that, for any neural network achieving zero loss, adversarial attacks arise in directions orthogonal to the data manifold. Then, we rely on the submanifold extension lemma [15] to show that in the limit of infinitely-wide layers, for any neural network and any weights set there exists another weights set (of the same neural network architecture) achieving the same loss and with opposite loss gradients orthogonal to the data manifold on a given point. Finally, by relying on the convergence of BNNs to Gaussian Processes (GPs) [6] and under the assumption that the data manifold is a subspace, we show that for infinitely-wide BNNs the expectation of the gradient w.r.t. the posterior distribution in a direction orthogonal to the data manifold vanishes. Crucially, our results guarantees that, in the limit, BNNs’ posteriors are provably robust to gradient-based adversarial attacks even when neural networks sampled from the posterior are vulnerable to such attacks.

We experimentally support our theoretical findings on various BNN architectures trained with Hamiltonian Monte Carlo (HMC) and with Variational Inference (VI) on MNIST, Fashion MNIST and the half moons datasets, empirically showing that the magnitude of the gradients decreases as more samples are taken from the BNN posterior. We then explore the robustness of BNNs to adversarial attacks experimentally in these settings. In particular, we conduct a large-scale experiment on thousands of different neural networks, empirically finding that, in the cases here analysed, for BNNs higher accuracy tend to correlate with higher robustness to gradient-based adversarial attacks,

contrary to what observed for deterministic NNs trained via standard Stochastic Gradient Descent (SGD). Finally, we also investigate the robustness of BNNs to gradient-free adversarial attacks, empirically showing that BNNs are substantially more robust than their deterministic counterpart even in this setting.

In summary, this paper makes the following contributions:

- A proof that, in the infinitely-wide layers and large data limit setting, the gradient of the loss function w.r.t. the input only preserves the component which is orthogonal to the data manifold (Section III) and that for any weights set of a neural network there exists another weight set with same loss and opposite orthogonal gradients (Section III-A).
- A proof that, in the infinitely-wide limit, for BNNs, the expected posterior gradient vanishes when projected in a direction orthogonal to the data manifold, thus providing robustness to BNNs (Section IV).
- Experiments showing empirically that BNNs are more robust to both gradient-based and gradient-free attacks than their deterministic counterpart and can resist the well known accuracy-robustness trade-off (Section VI).¹

A preliminary version of this work appeared in [16]. This work extends [16] in several aspects. In [16] we proved that given an infinitely-wide neural network with zero loss and a non-zero orthogonal gradient to the data manifold, there exists another zero-loss neural network with opposite orthogonal gradient and use this result to conjecture that BNNs achieve zero gradients in expectation under a wide enough prior. In this paper, in Section IV this conjecture is shown to be true and proved explicitly. Furthermore, we substantially extend the discussion and the theoretical analysis, and improve the empirical results with gradient-free adversarial attacks.

The paper is structured as follows. In Section II we introduce background on infinitely-wide neural networks and BNNs. In Section III we will first show that for highly accurate neural networks the gradient of the loss is non-zero only in directions orthogonal to the data manifold. Then, in Section III-A we will prove that for any neural network and weight set there exists another weight set of the same neural network with same loss and opposite orthogonal gradients to the data manifold. By averaging over these weight sets and relying on the convergence of BNNs to Gaussian processes (GPs), in Section IV we prove that for a BNN that achieves zero loss on the data manifold the expected gradient of the loss is zero, thus making them robust to adversarial attacks. Section V discusses consequences and limitations of our results. Empirical results in Section VI will support our theoretical findings.

A. Related Work

Adversarial attacks for deterministic neural networks have been the subject of extensive analyses [17, 18, 19, 20, 21, 22, 23], which have led to the development of multiple defence and attack methods over the recent years [4]. Adversarial examples have been found to be so widespread in state-of-the-art deterministic NNs that they have even been hypothesized to

¹The code for the experiments can be found at <https://github.com/ginevracoal/robustBNNs>.

be an intrinsic property of certain models [22] or datasets [24]. Interestingly, early experimental results with BNNs suggested a diametrically different behaviour than that of their deterministic counter-part. In fact, empirical observations on the increased adversarial robustness of BNNs have been made in various works both against gradient-based adversarial attacks [25, 26, 27] and gradient-free adversarial attacks [14] as well as on reinforcement learning settings [28]. However, while these works present empirical evidences on the robustness of BNNs, they do not give any theoretical justification on the mechanisms that lead to BNN robustness. First attempts to understand the robustness properties of BNNs have been considered in [12, 29]. In particular, [12] defined Bayesian adversarial spheres and empirically showed that, for BNNs trained with HMC, adversarial examples tend to have high uncertainty. Instead [29] derived sufficient conditions for idealised BNNs to avoid adversarial examples. However, it is unclear how such conditions could be checked in practice, as it would require one to check that the BNN architecture is invariant under all the symmetries of the data.

Because of the capabilities of BNNs to model epistemic uncertainty, which can be intuitively linked to their robustness properties, various approaches have been proposed to detect adversarial examples for BNNs. [10, 30] propose to use the uncertainty on the predictions of a BNN as a way to flag adversarial attacks. However, such methods have been shown to be easily fooled by appropriately crafted adversarial attacks [31, 32]. Consequently, formal verification methods [33, 34] to detect adversarial examples for BNNs have been introduced. These methods have been followed by techniques to perform adversarial training for BNNs [35, 36, 13, 11], where additional robustness constraints or penalties are considered directly at training time. Interestingly, empirical results obtained with such techniques, highlighted how, in the Bayesian settings, high accuracy and high robustness often are positively correlated with each other. The theoretical framework we develop in this paper further confirms and grounds these findings.

II. BACKGROUND

Let $f^{true} : \mathcal{M} \rightarrow \mathbb{R}$ be a function defined on a data manifold $\mathcal{M} \subseteq X \subseteq \mathbb{R}^d$ with X being the ambient (or embedding) space.² We consider the problem of approximating f^{true} via the learning of an $M + 1$ layers neural network $f(\cdot, \mathbf{w})$, with $\mathbf{w} \in \mathbb{R}^{n_w}$ being the aggregate vector of weights and biases. Formally, for $\mathbf{x} = (x_1, \dots, x_d) \in X$, $f(\mathbf{x}, \mathbf{w})$ is defined iteratively over the number of layers as:

$$f_i^{(1)}(\mathbf{x}) = \sum_{j=1}^d w_{ij}^{(1)} x_j + b_i^{(1)} \quad (1)$$

$$f_i^{(m)}(\mathbf{x}) = \sum_{j=1}^{n_{m-1}} w_{ij}^{(m)} \phi(f_j^{(m-1)}(\mathbf{x})) + b_i^{(m)}, \quad (2)$$

$$f(\mathbf{x}, \mathbf{w}) = f^{(M+1)}(\mathbf{x}), \quad (3)$$

²For simplicity of presentation, we assume a scalar output. The results of this paper naturally extend to the multi-output case by treating each output component similarly to the single output case.

for $m = 2, \dots, M + 1$, where n_m is the number of neurons in the m -th layer and ϕ is the activation function – which we assume to be continuous. In order to learn the weights of $f(\mathbf{x}, \mathbf{w})$ one considers a dataset D_N composed of N points, $D_N = \{(\mathbf{x}_i, y_i) \mid \mathbf{x}_i \in \mathcal{M}, y_i = f^{true}(\mathbf{x}_i), i = 1, \dots, N\}$. In a frequentist fashion, one can then use the dataset to quantify the distance between f^{true} and $f(\cdot, \mathbf{w})$ by evaluating it on a loss function $L(\mathbf{x}, \mathbf{w})$ of the form $L(\mathbf{x}, \mathbf{w}) = \ell(f(\mathbf{x}, \mathbf{w}), f^{true}(\mathbf{x}))$, with $\ell(\cdot, \cdot)$ chosen accordingly to the semantic of the problem at hand (e.g., square loss or cross-entropy).³ Intuitively, minimisation of the loss function over the weight vector \mathbf{w} leads to increasing fit of $f(\mathbf{x}, \mathbf{w})$ to $f^{true}(\mathbf{x})$, with zero-loss indicating that the fit is exact [37] on D_N .

In this paper, we aim at analysing the adversarial robustness of $f(\mathbf{x}, \mathbf{w})$. In order to do so, we will rely on crucial results from Bayesian learning of neural networks and on the properties of infinitely-wide neural networks. The remainder of this section is dedicated to the review of such notions.

A. Infinitely-Wide Neural Networks

In our analysis we will rely on the notion of infinitely-wide NNs, i.e. NNs with an infinite number of neurons.

Definition 1 (Infinitely-wide neural network). *Consider a family of neural networks $\{f(\mathbf{x}, \mathbf{w}_{n_w})\}_{n_w > 0}$ of Equations (1)–(3), with a fixed number of neurons for $m = 1, \dots, M - 1$ and a variable number of neurons n_M in the last hidden layer. We say that*

$$f^\infty(\mathbf{x}) := \lim_{n_M \rightarrow \infty} f(\mathbf{x}, \mathbf{w}_{n_w}) \quad \forall \mathbf{x} \in X, \quad (4)$$

is an infinitely wide neural network if the limit above exists and if the resulting function defines a mapping from X to \mathbb{R} . Furthermore, we call \mathcal{F} the set of such limit functions.

The interest behind the set of infinitely-wide neural networks lies in the fact that they are universal approximators [38, 39].⁴ More precisely, under the assumption that the true function f^{true} is continuous, we have that:

$$\forall \epsilon > 0, \exists f^* \in \mathcal{F} \text{ s.t. } \forall \mathbf{x} \in \mathcal{M}, \quad |f^{true}(\mathbf{x}) - f^*(\mathbf{x})| < \epsilon. \quad (5)$$

That is, \mathcal{F} is dense in the space of continuous functions. Furthermore, it is possible to show that any smooth function with bounded derivatives can be represented exactly by an infinitely wide NN with bounded weights norm (i.e. with bounded sum of the squared Euclidean norm of the weights in the network) [41]. We will rely on these crucial properties of infinitely-wide neural networks to reason about their behaviour against adversarial attacks. We remark that the existence of such a neural network f^* approximating the true underlying function does not necessarily mean that it will be automatically found through gradient descent-based training on a finite

³For simplicity of notation we omit the explicit dependence on the true function from the loss.

⁴Notice that the limit in Definition 1 is taken only w.r.t. the last hidden layer. Similar results, albeit with additional care needed for the definition of the limiting sequence, can be obtained by taking the limit w.r.t. all the hidden layers [40].

dataset. However, recent results [42] have shown that, under mild conditions, the loss function, as a functional over the distribution over weights of an infinitely-wide NN, is a convex functional, and hence the gradient flow of stochastic gradient descent will converge to a unique distribution over weights. That is, given an infinitely-wide NN f^∞ and a sequence of datasets $\{D_N\}_{N > 0}$ of cardinality N extracted from the data manifold \mathcal{M} , we have that:

$$\lim_{N \rightarrow \infty} \ell(f_{D_N}^\infty(\mathbf{x}), f^{true}(\mathbf{x})) = 0, \quad \forall \mathbf{x} \in \mathcal{M} \quad (6)$$

where $f_{D_N}^\infty$ represents the infinitely-wide NN trained on D_N until convergence. In Section III we will show how infinitely-wide deterministic neural networks, i.e., neural networks where each weight or bias is a scalar, can be vulnerable to adversarial attacks even when the loss is zero, while infinitely-wide Bayesian neural networks, under certain assumptions on the geometry of the data manifold, are provably robust to gradient-based adversarial attacks.

B. Bayesian Neural Networks

Bayesian modelling aims to capture the uncertainty of data driven models by defining ensembles of predictors [43]; it does so by turning model parameters into random variables. In the NN scenario, one starts by putting a prior measure over the network weights $p(\mathbf{w})$ [6].⁵ The fit of the network with weights \mathbf{w} to the data D is assessed through the likelihood $p(D|\mathbf{w})$ [44].⁶ Bayesian inference then combines likelihood and prior via the Bayes theorem to obtain a *posterior* distribution over the NN parameters

$$p(\mathbf{w}|D) \propto p(D|\mathbf{w}) p(\mathbf{w}). \quad (7)$$

Unfortunately, it is in general infeasible to compute the posterior distribution exactly for non-linear/non-conjugate models such as deep NNs, so that approximate Bayesian inference methods are employed in practice. Asymptotically exact samples from the posterior distribution can be obtained via procedures such as Hamiltonian Monte Carlo (HMC) [45], while approximate samples can be obtained more cheaply via Variational Inference (VI) [46]. Irrespective of the posterior inference method of choice, Bayesian empirical predictions at a new input \mathbf{x} are obtained from an ensemble of n NNs, each with its individual weights drawn from the posterior distribution $p(\mathbf{w}|D)$:

$$\langle f(\mathbf{x}, \mathbf{w}) \rangle_{p(\mathbf{w}|D)} \simeq \frac{1}{n} \sum_{i=1}^n f(\mathbf{x}, \mathbf{w}_i) \quad (8)$$

where $\mathbf{w}_i \sim p(\mathbf{w}|D)$ and $\langle \cdot \rangle_{p(\mathbf{w}|D)}$ denotes expectation w.r.t. the posterior distribution $p(\mathbf{w}|D)$.

Note that the definition of a distribution over the weights $p(\mathbf{w})$ naturally leads to the definition of a probability measure over the set of continuous functions $f : \mathbb{R}^d \rightarrow \mathbb{R}$ that can be

⁵In the remainder of this paper, we employ the common notation of indicating density functions with p and their corresponding probability measures with P .

⁶Notice that in the Bayesian setting the likelihood is a transformation of the loss function used in deterministic settings. In the rest of the paper we use both terminologies, and the loss is not to be confused with that used in Bayesian decision theory [44].

represented by the neural network. In particular, as common in the literature [47, 48], we consider the probability measure P generated by the finite-dimensional distributions of the BNN, i.e., the joint distributions of $f(\mathbf{x}_1, \mathbf{w}), \dots, f(\mathbf{x}_k, \mathbf{w})$, where k is an arbitrary integer and $\mathbf{x}_1, \dots, \mathbf{x}_k \in X$. We stress that in general not all path properties, such as continuity or differentiability, can be determined using the finite dimensional distributions. However, as the neural networks architectures considered in this paper are continuous by assumption, without any lost of generality and as common in the literature [47], we assume that $f(\cdot, \mathbf{w})$ is separable, i.e., countable dense subsets of input points suffice to determine the properties of $f(\cdot, \mathbf{w})$.

In this paper, as also common in the literature [46], we will consider Gaussian priors $p(\mathbf{w})$. The following result shows how an independent Gaussian prior over the parameters of an infinitely-wide BNN induces a Gaussian prior over the space of functions.

Proposition 1 ([6, 40]). *Consider the following neural network $f(\mathbf{x}, \mathbf{w})$ with a single hidden-layer defined as*

$$f_i^{(1)}(\mathbf{x}) = \sum_{j=1}^d w_{ij}^{(1)} x_j + b_i^{(1)} \quad (9)$$

$$f_i^{(2)}(\mathbf{x}) = \sum_{j=1}^{n_1} w_{ij}^{(2)} \phi(f_j^{(m-1)}(\mathbf{x})) + b_i^{(2)}, \quad (10)$$

$$f(\mathbf{x}, \mathbf{w}) = f^{(2)}(\mathbf{x}). \quad (11)$$

Assume that to each weight and bias are associated independent normal priors such that $w_{ij}^{(1)} \sim \mathcal{N}(0, \frac{\sigma_w^2}{d})$, $w_{ij}^{(2)} \sim \mathcal{N}(0, \frac{\sigma_w^2}{n_1})$, $b_i^{(1)}, b_i^{(2)} \sim \mathcal{N}(0, \sigma_b^2)$. Then, for $n_1 \rightarrow \infty$, the prior on $f_i(\mathbf{x}, \mathbf{w})$ converges in distribution to a Gaussian process (GP) with zero mean and covariance function $K(\mathbf{x}, \mathbf{x}') = \sigma_b^2 + \sigma_w^2 C(\mathbf{x}, \mathbf{x}')$, where $C(\mathbf{x}, \mathbf{x}')$ is a function dependent on the BNN architecture.

Note that, while Proposition 1 is stated only for BNNs with one hidden layer, analogous results can be derived for the multiple hidden layer case and also for more complex architectures such as convolutional neural networks [40, 49, 50]. We stress that in the case of multiple hidden layers, care must be taken in how the size of the various layers goes to infinity to guarantee convergence. In what follows, we will simply assume that for an infinitely-wide BNN, the conditions for convergence are always satisfied.

Thanks to Proposition 1 we have that an infinitely-wide BNN is equivalent to a GP. This allows us to use the favourable analytical properties of GPs to study BNN robustness in the limit. In particular, in Section IV we will rely on the fact that the (mean-square) derivative⁷ of a GP is still a GP with a kernel given by the derivative of the kernel of the original GP [47]. This is a key result that we will use to show how the orthogonal gradient of the loss for trained BNNs vanishes along the data manifold.

⁷In this paper we will always focus on mean-square derivatives for probabilistic models. Hence, in what follows, we will simply refer to them as derivatives.

C. Adversarial Attacks for Bayesian Neural Networks

Given an input point $\mathbf{x} \in \mathcal{M}$ and a strength (i.e. maximum perturbation magnitude) $\epsilon > 0$, the worst-case adversarial perturbation can be defined as the point $\tilde{\mathbf{x}}$ in the ϵ -neighbourhood around \mathbf{x} that maximises the loss function L :

$$\tilde{\mathbf{x}} := \arg \max_{\tilde{\mathbf{x}}: \|\tilde{\mathbf{x}} - \mathbf{x}\| \leq \epsilon} \langle L(\tilde{\mathbf{x}}, \mathbf{w}) \rangle_{p(\mathbf{w}|D)}.$$

If the network prediction on $\tilde{\mathbf{x}}$ differs from the original prediction on \mathbf{x} , then we call $\tilde{\mathbf{x}}$ an *adversarial example*. As $f(\mathbf{x}, \mathbf{w})$ is non-convex, computing $\tilde{\mathbf{x}}$ is a non-convex optimisation problem for which several approximate solution methods have been proposed. In this paper we will primarily focus on what arguably is the most commonly employed class among them, i.e., gradient-based attacks, that is attacks that employ the loss function gradient w.r.t. \mathbf{x} to maximise the loss [4]. One such attacks is the Fast Gradient Sign Method (FGSM) [2] which works by approximating $\tilde{\mathbf{x}}$ by taking an ϵ -step in the direction of the sign of the gradient at \mathbf{x} . In the context of BNNs, where attacks are against the posterior distribution, applying FGSM yields

$$\tilde{\mathbf{x}} = \mathbf{x} + \epsilon \operatorname{sgn} \langle \nabla_{\mathbf{x}} L(\mathbf{x}, \mathbf{w}) \rangle_{p(\mathbf{w}|D)} \quad (12)$$

$$\simeq \mathbf{x} + \epsilon \operatorname{sgn} \left(\sum_{i=1}^n \nabla_{\mathbf{x}} L(\mathbf{x}, \mathbf{w}_i) \right) \quad (13)$$

where the final expression is a Monte Carlo approximation with n samples \mathbf{w}_i drawn from the posterior $p(\mathbf{w}|D)$. Other gradient-based attacks, as for example Projected Gradient Descent method (PGD) [5], modify FGSM by taking consecutive gradient iterations or by scaling the attack by the magnitude of the gradient. Crucially, however, they all rely on the gradient vector to guide the attack.

In the following sections we will rely on the fact that the expected loss gradient in Equation (12) can be decomposed into its projection into a direction parallel to the data manifold and into a direction orthogonal to the data manifold. The parallel expected loss gradient naturally vanishes for very accurate neural neural networks as the loss will tend to be zero everywhere in the data manifold. Instead, the orthogonal projection will in general not be zero. However, perhaps surprisingly, we will show that for infinitely-wide Bayesian neural network also the orthogonal expected loss gradient vanishes.

Before considering results specific to BNNs in Section IV, in Section III we will focus on results that hold for both deterministic and Bayesian neural networks (Lemma 1) and that are specific to deterministic NNs (Proposition 2), showing how these can be vulnerable to adversarial attacks even when they learn the true function perfectly.

III. GRADIENT-BASED ADVERSARIAL ATTACKS FOR NEURAL NETWORKS

Equation (12) suggests a possible mechanism through which BNNs might acquire robustness against adversarial attacks: averaging under the posterior might lead to cancellations in the expectation of the gradient of the loss. It turns out that this averaging property is intimately related to the geometry

of the data manifold \mathcal{M} . As a consequence, in order to study the expectation of the gradient of the loss for BNNs, we first introduce results that link the geometry of \mathcal{M} to adversarial attacks.

We start with a trivial, yet important result, which holds for any neural network, both Bayesian and deterministic: for a NN that achieves zero loss on the whole data manifold \mathcal{M} , the loss gradient is constant (and zero) along the data manifold for any $\mathbf{x} \in \mathcal{M}$. Therefore, in order to have adversarial examples the dimension of the data manifold \mathcal{M} must necessarily be smaller than the dimension of the ambient space, that is, $\dim(\mathcal{M}) < \dim(X) = d$, where $\dim(\mathcal{M})$ denotes the dimension of \mathcal{M} .

Lemma 1. *Assume that \mathcal{M} is a smooth closed manifold and that $\forall \mathbf{x} \in \mathcal{M} L(\mathbf{x}, \mathbf{w}) = 0$, that is $f(\mathbf{x}, \mathbf{w})$ achieves zero loss on \mathcal{M} . Then, if f is vulnerable to gradient-based attacks at $\mathbf{x}^* \in \mathcal{M}$, $\dim(\mathcal{M}) < \dim(X)$ in a neighbourhood of \mathbf{x}^* , i.e. \mathcal{M} is locally homeomorphic to a space of dimension smaller than the ambient space X .*

Proof. By assumption $\forall \mathbf{x} \in \mathcal{M}, L(\mathbf{x}, \mathbf{w}) = 0$, which implies that the gradient of the loss is zero along the data manifold. However, if f is vulnerable to gradient based attacks at \mathbf{x}^* then the gradient of the loss at \mathbf{x}^* must be non-zero. Hence, there exists an open neighbourhood \mathcal{B} of \mathbf{x}^* such that $\mathcal{B} \not\subseteq \mathcal{M}$, which implies $\dim(\mathcal{M}) < \dim(X)$ locally around \mathbf{x}^* . \square

Lemma 1 confirms the widely held conjecture that adversarial attacks may originate from degeneracies of the data manifold [2, 51]. In fact, it has been already empirically noticed [52] that adversarial perturbations often arise in directions normal to the data manifold. The suggestion that lower-dimensional data structures might be ubiquitous in NN problems is also corroborated by recent results [53] showing that the characteristic training dynamics of NNs are intimately linked to data lying on a lower-dimensional manifold. Notice that the implication is only one way; it is perfectly possible for the data manifold to be low dimensional and still not vulnerable at many points.

We note that, as discussed in Section II-A, at convergence of the training algorithm and in the limit of infinitely-many data, infinitely-wide neural networks are guaranteed to achieve zero loss on the data manifold, satisfying the assumption of Lemma 1. As a result, once an infinitely-wide NN is fully trained, for any $\mathbf{x} \in \mathcal{M}$ the gradient of the loss function is orthogonal to the data manifold as it is zero along the data manifold, i.e., $\nabla_{\mathbf{x}} L(\mathbf{x}, \mathbf{w}) = \nabla_{\mathbf{x}}^{\perp} L(\mathbf{x}, \mathbf{w})$, where $\nabla_{\mathbf{x}}^{\perp}$ denotes the gradient projected into the normal subspace of \mathcal{M} at \mathbf{x} . We stress that for a given NN, $\nabla_{\mathbf{x}}^{\perp} L(\mathbf{x}, \mathbf{w})$ is in general non-zero even if the network achieves zero loss on \mathcal{M} (this is formalized in the next subsection), thus explaining the existence of adversarial examples even for very accurate classifiers. Crucially, in Section IV we show that for BNNs, when averaged w.r.t. the posterior distribution, the orthogonal gradient vanishes.

A. A Symmetry Property of Neural Networks

Before considering the BNN case, in Proposition 2 below we show a symmetry property of neural networks: given a neural network, we can always find an infinitely-wide NN that has the same loss but opposite orthogonal gradient. In order to

prove this result, we first introduce Lemma 2, which is a generalization of the submanifold extension lemma and a key result we leverage. It proves that any smooth function defined on a submanifold \mathcal{M} can be extended to the ambient space, in such a way that the choice of the derivatives orthogonal to the submanifold is arbitrary.

Lemma 2 ([54]). *Assume that \mathcal{M} is a smooth closed manifold. Let $T_{\mathbf{x}}\mathcal{M}$ be the tangent space of \mathcal{M} at a point $\mathbf{x} \in \mathcal{M}$. Let $V = \sum_{i=\dim(\mathcal{M})+1}^d v^i \partial_i$ be a conservative vector field along \mathcal{M} which assigns a vector in $T_{\mathbf{x}}\mathcal{M}^{\perp}$ for each $\mathbf{x} \in \mathcal{M}$. For any smooth function $f^{\text{true}} : \mathcal{M} \rightarrow \mathbb{R}$ there exists a smooth extension $F : X \rightarrow \mathbb{R}$ such that*

$$F|_{\mathcal{M}} = f^{\text{true}},$$

where $F|_{\mathcal{M}}$ denotes the restriction of F to the submanifold \mathcal{M} , and such that the derivative of the extension F is

$$\nabla_{\mathbf{x}} F(\mathbf{x}) = (\nabla_1 f^{\text{true}}(\mathbf{x}), \dots, \nabla_{\dim(\mathcal{M})} f^{\text{true}}(\mathbf{x}), \\ v^{\dim(\mathcal{M})+1}(\mathbf{x}), \dots, v^d(\mathbf{x}))$$

for all $\mathbf{x} \in \mathcal{M}$.

Notice that in Lemma 2, in $\nabla_{\mathbf{x}} F(\mathbf{x})$, we pick the local coordinates at $\mathbf{x} \in \mathcal{M}$, such that the first set of components parametrises the data manifold. We stress that, as \mathcal{M} is smooth, this is without any loss of generality [15]. Lemma 2, together with the universal approximation capabilities of NNs [39], is employed in Proposition 2 to show that for any possible value \mathbf{v} of the orthogonal gradient to the data manifold in a point, there exists at least two (possibly not unique) different weight vectors that achieve zero loss and have orthogonal gradients respectively equal to \mathbf{v} and $-\mathbf{v}$.

Proposition 2. *Consider an infinitely-wide NN f with smooth, bounded, and non-constant activation functions and an input $\mathbf{x} \in \mathcal{M}$, where \mathcal{M} is a smooth closed manifold. Then, for any smooth function $f^{\text{true}} : \mathcal{M} \rightarrow \mathbb{R}$ and vector $\mathbf{v} \in \mathbb{R}^{\dim(X) - \dim(\mathcal{M})}$, there exist $\mathbf{w}_1, \mathbf{w}_2$ such that*

$$f(\cdot, \mathbf{w}_1)|_{\mathcal{M}} = f^{\text{true}} = f(\cdot, \mathbf{w}_2)|_{\mathcal{M}} \quad (14)$$

$$\nabla_{\mathbf{x}}^{\perp} f(\mathbf{x}, \mathbf{w}_1) = \mathbf{v} = -\nabla_{\mathbf{x}}^{\perp} f(\mathbf{x}, \mathbf{w}_2). \quad (15)$$

Proof. From Lemma 2 we know that there exist smooth extensions F^+ and F^- of f^{true} to the embedding space such that $\nabla_{\mathbf{x}}^{\perp} F^+(\mathbf{x}) = \mathbf{v} = -\nabla_{\mathbf{x}}^{\perp} F^-(\mathbf{x})$. As a consequence, to conclude the proof it suffices to apply Theorem 3 in [39] that guarantees that infinitely-wide neural networks are *uniformly 1-dense* on compacts in $\mathcal{C}^1(X)$, under the assumptions of smooth, bounded, and non-constant activation functions. Specifically, for any $F \in \mathcal{C}^1(X)$ and $\epsilon > 0$, for any compact $X' \subseteq X$ there exists a set of weights \mathbf{w} s.t.

$$\max \left\{ \sup_{\mathbf{x} \in X'} ||F(\mathbf{x}) - f(\mathbf{x}, \mathbf{w})||_{\infty}, \sup_{\mathbf{x} \in X'} ||\nabla F(\mathbf{x}) - \nabla f(\mathbf{x}, \mathbf{w})||_{\infty} \right\} \leq \epsilon.$$

As $F^+, F^- \in \mathcal{C}^1(X)$, this concludes the proof. \square

Note that by the chain rule, the gradient of the loss is proportional to the gradient of the NN. As a consequence, Proposition 2 guarantees that, for infinitely-wide NNs, for any weights set achieving the minimum loss, there exists another weights set with same loss and opposite orthogonal gradient of the loss w.r.t. the input. This has various implications: i) deterministic NNs trained on a data manifold could exhibit arbitrarily large gradients in directions orthogonal to the data manifold, even when they learn the latent function perfectly, ii) in a Bayesian framework, by averaging over weights sets that have opposite orthogonal gradients, one could achieve a robust model that has vanishing expected orthogonal gradient. In the next Section, in Theorems 1 and 2 we show that, under some relatively mild assumptions, this is indeed the case. However, we should already emphasize that such a result does not hold by simply averaging the set of weights w.r.t. any distribution. Intuitively, for this result to hold, it is required that each set of weights achieving a given gradient value has the same measure as the set of weights with the same loss and opposite orthogonal gradient value.

IV. ADVERSARIAL ROBUSTNESS VIA BAYESIAN AVERAGING

In order to prove that BNNs have vanishing orthogonal gradients, we start from a general Gaussian process [55] trained with a given dataset. We show that, under the assumption that the data manifold is a linear subspace of the ambient space, the projection of the expected gradient of the GP in a direction orthogonal to the data manifold vanishes for all points in the data manifold, showing how GPs are able to obtain perfect cancellation of the orthogonal gradients. By relying on the convergence of BNNs to GPs we then extend this result to infinitely-wide (trained) BNNs.

We first state our results for a regression setting, the classification setting will then be considered in Section IV-A.

Theorem 1. *Let $z(\mathbf{x})$ be a zero-mean Gaussian process with covariance function $K : \mathbb{R}^d \times \mathbb{R}^d \rightarrow \mathbb{R}$. Call $z(\mathbf{x}) | D_N$ the posterior GP obtained by training z on a regression problem with data set $D_N = \{(\mathbf{x}_i, \mathbf{y}_i) | i = 1, \dots, N\}$ and additive zero mean Gaussian observation noise of variance $\sigma^2 \geq 0$. Assume that:*

- For $\mathbf{x}', \mathbf{x}'' \in \mathcal{M}$, $K(\mathbf{x}', \mathbf{x}'') = g(\sum_{i=1}^d (x'_i - x''_i)^l)$, $l > 1$ or $K(\mathbf{x}', \mathbf{x}'') = g(\sum_{i=1}^d x'_i x''_i)$, where g is any twice differentiable function such that K is a valid kernel.
- \mathcal{M} is a linear subspace of $X \subseteq \mathbb{R}^d$.

Then, for any $\mathbf{x} \in \mathcal{M}$ it holds that

$$\langle \nabla_{\mathbf{x}}^{\perp} z(\mathbf{x}) \rangle_{p(z(\mathbf{x}) | D_N)} = 0. \quad (16)$$

Proof. Conditional distributions of jointly Gaussian random variables are still Gaussian [56]. Consequently, $z | D_N$ is a Gaussian process with mean at \mathbf{x} given by

$$\langle z(\mathbf{x}) \rangle_{p(z(\mathbf{x}) | D_N)} = K(\mathbf{x}, X) (K(X, X) + \sigma^2 I)^{-1} [\mathbf{y}_1, \dots, \mathbf{y}_N]^T, \quad (17)$$

where

$$K(\mathbf{x}, X) = [K(\mathbf{x}, \mathbf{x}_1), \dots, K(\mathbf{x}, \mathbf{x}_N)]$$

$$K(X, X) = \begin{bmatrix} K(\mathbf{x}_1, \mathbf{x}_1) & \dots & K(\mathbf{x}_1, \mathbf{x}_N) \\ \vdots & \ddots & \vdots \\ K(\mathbf{x}_N, \mathbf{x}_1) & \dots & K(\mathbf{x}_N, \mathbf{x}_N) \end{bmatrix}.$$

As the derivative of a Gaussian process is still a Gaussian process with mean given by the derivative of its mean [56], by the linearity of the expectation and the definition of vector projection, we obtain that

$$\langle \nabla_{\mathbf{x}}^{\perp} z(\mathbf{x}) \rangle_{p(z(\mathbf{x}) | D_N)} = \quad (18)$$

$$\left(\sum_{i=1}^d v_i \frac{\partial K(\mathbf{x}, \mathbf{x}_i)}{\partial x_i} \right) (K(X, X) + \sigma^2 I)^{-1} [\mathbf{y}_1, \dots, \mathbf{y}_N]^T \cdot \mathbf{v}, \quad (19)$$

where $\mathbf{v} = (v_1, \dots, v_d)$ is a unit vector orthogonal to \mathcal{M} in \mathbf{x} , which always exists if $\dim(\mathcal{M}) < \dim(X)$, and I is the identity matrix of size equal to $K(X, X)$. Hence, if we can show that for any $\mathbf{x}' \in \mathcal{M}$, $\sum_{i=1}^d v_i \frac{\partial K(\mathbf{x}, \mathbf{x}')}{\partial x_i} = 0$, then the proof is concluded. In order to do that, we notice that, as \mathcal{M} is a subspace, the orthogonal direction \mathbf{v} is a vector of the orthogonal complement of \mathcal{M} . Consequently, it holds that

$$\forall \mathbf{x} \in \mathcal{M}, \quad \sum_{i=1}^d v_i x_i = 0.$$

From this, for the case $K(\mathbf{x}, \mathbf{x}') = g(\sum_{i=1}^d x_i x'_i)$, we obtain that for any $\mathbf{x}' \in \mathcal{M}$ it holds that

$$\begin{aligned} \sum_{i=1}^d v_i \frac{\partial K(\mathbf{x}, \mathbf{x}')}{\partial x_i} &= \\ \sum_{i=1}^d v_i g' \left(\sum_{j=1}^d x_j x'_j \right) x'_i &= \\ g' \left(\sum_{i=1}^d x_i x'_i \right) \left(\sum_{i=1}^d v_i x'_i \right) &= 0. \end{aligned}$$

The case $K(\mathbf{x}, \mathbf{x}') = g(\sum_{i=1}^d (x_i - x'_i)^l)$ follows similarly using the fact that subspaces are closed under linear combination. \square

Corollary 1. *Let $f(\mathbf{x}, \mathbf{w})$ be a BNN trained on a regression problem with data set $D_N = \{(\mathbf{x}_i, \mathbf{y}_i) | i = 1, \dots, N\}$ with additive zero mean Gaussian observation noise of variance σ^2 . Assume that:*

- To each weight and bias are associated independent normal priors.
- \mathcal{M} is a linear subspace of $X \subseteq \mathbb{R}^d$.

Then, for any $\mathbf{x} \in \mathcal{M}$, for an infinitely-wide BNNs it holds that

$$\langle \nabla_{\mathbf{x}}^{\perp} f(\mathbf{x}) \rangle_{p(f(\mathbf{x}, \mathbf{w}) | D_N)} = 0. \quad (20)$$

Proof. In the limit of infinitely-wide architecture, thanks to Proposition 1, $f(\mathbf{x}, \mathbf{w})$ converges weakly to a GP. However, in general, the resulting kernel will not directly match the kernels satisfying the assumption of Theorem 1. Rather, in the case of BNNs with fully connected architectures, it will be of the form [40]⁸

$$K(\mathbf{x}, \mathbf{x}') = g(\mathbf{x}\mathbf{x}', \mathbf{x}'\mathbf{x}'),$$

⁸Note that the result also holds for convolutional BNNs where for the convolutional kernel instead, each monomial could be weighted differently depending on the number of filters, size and stride of the kernel.

where $\mathbf{x}\mathbf{x}'$ is the dot product between vectors \mathbf{x} and \mathbf{x}' . However, by the chain rule for multivariable functions, we get that

$$\begin{aligned} \frac{\partial K(\mathbf{x}, \mathbf{x}')}{\partial x_i} &= \\ 2x_i D_1[g(\mathbf{xx}, \mathbf{xx}', \mathbf{x}'\mathbf{x}')] + x'_i D_2[g(\mathbf{xx}, \mathbf{xx}', \mathbf{x}'\mathbf{x}')], \end{aligned} \quad (21)$$

where $D_i[g]$ indicates the partial derivative of function g w.r.t. argument i . Consequently, being both \mathbf{x} and \mathbf{x}' in the data manifold \mathcal{M} , the derivations in the proof of Theorem 1 apply to each of the argument of Eqn (21). To conclude the proof it is enough to notice that Proposition 1 in [57] guarantees that the BNN posterior converges weakly to the posterior induced by the GP limit of the prior. Consequently, being the operator

$$\mathcal{G}_{\mathbf{x}} : f \mapsto \nabla_{\mathbf{x}}^{\perp} f(\mathbf{x}),$$

linear and bounded by assumption, we have that

$$\langle \nabla_{\mathbf{x}}^{\perp} f(\mathbf{x}) \rangle_{p(f(\mathbf{x}, \mathbf{w})|D_N)} \rightarrow \langle \nabla_{\mathbf{x}}^{\perp} z(\mathbf{x}) \rangle_{p(z(\mathbf{x})|D_N)} = 0,$$

where $\langle \nabla_{\mathbf{x}}^{\perp} z(\mathbf{x}) \rangle_{p(z(\mathbf{x})|D_N)}$ is as defined in Theorem 1. \square

Note that the assumptions on K are relatively mild. In fact, by Corollary 1 not only they include the kernels given by the limiting GP of most common BNN architectures including also convolutional neural networks [58], but they are also satisfied by most kernels used in practice for learning with GPs. Consequently, our results also apply to recent approaches that encode informative functional priors for BNNs as Gaussian processes [59].

We should also stress that Theorem 1 and Corollary 1 hold for any size of D_N . Of course, in this general setting, the projection of the expected gradient of the loss to a direction parallel to \mathcal{M} may not be zero, but will only necessarily point to directions where the loss increases within the data manifold. Consequently, if a BNN has small loss everywhere in the data manifold, then necessarily $\langle \nabla_{\mathbf{x}}^{\perp} f(\mathbf{x}) \rangle_{p(f(\mathbf{x}, \mathbf{w})|D_N)}$ will vanish for any $\mathbf{x} \in \mathcal{M}$.

Remark 1. In Theorem 1 we only consider the expectation of the orthogonal gradient. However, Theorem 1 does not imply that also the variance of the orthogonal projection of the GP vanishes. In fact, in general, the variance is non-zero, showing how the robustness properties occur only in expectation. To investigate this, in Figure 1 we consider a synthetic regression example, where the ambient space is \mathbb{R}^2 and the data manifold is the line $x_1 = x_2$ and on the same data generated by a non-linear function we train both a BNN with HMC and the corresponding limiting GP, as well as a deterministic NN trained with stochastic gradient descent (SGD). For each point in the ambient space we compute the variance and mean of the scalar projection of the expected posterior gradient into a direction orthogonal to the data manifold. We observe that the variance is always non-vanishing on the ambient space, i.e., both inside and outside the data manifold. Furthermore, while for GPs and BNNs the mean of the orthogonal projection is respectively zero and approximately zero in the data manifold, for the DNN this is not always the case. Furthermore, the

absolute value of the expected orthogonal projection in any point in the ambient space is substantially greater for the DNN than for the GP and BNN.

Remark 2. The assumption that \mathcal{M} is a linear subspace is only needed to guarantee that all training points are orthogonal to the same vector defining the orthogonal direction in \mathbf{x} . This guarantees perfect cancellation. However, in the more general case, where \mathcal{M} is not a linear subspace, we expect that Theorem 1 and Corollary 1 can still approximately hold. In fact, for many kernels only training points close to the test point \mathbf{x} will influence the prediction at \mathbf{x} . Consequently, for the cancellation in Theorem 1 to hold it would be enough that the orthogonal direction in \mathbf{x} remains approximately orthogonal only in a neighbourhood of \mathbf{x} ; thus extending our result to more general \mathcal{M} .

A. Extension to Classification Setting

Theorem 1 is stated for regression, which is a particularly favourable setting for analysis because of the existence of closed form solutions for the GP posterior. Fortunately, in Theorem 2 and Corollary 2 below, we show that our results also extend to classification.

Theorem 2. Let $z(\mathbf{x})$ be a zero-mean Gaussian process (GP) with covariance function $K : \mathbb{R}^d \times \mathbb{R}^d \rightarrow \mathbb{R}$. Call $z(\mathbf{x})|D_N$ the posterior GP obtained by training z on a classification problem with data set $D_N = \{(\mathbf{x}_i, y_i) | i = 1, \dots, N, y_i \in \{0, 1\}\}$. Then, under the same assumptions of Theorem 1, for any $\mathbf{x} \in \mathcal{M}$ it holds that

$$\langle \nabla_{\mathbf{x}}^{\perp} z(\mathbf{x}) \rangle_{p(z(\mathbf{x})|D_N)} = 0. \quad (22)$$

Proof. Because of the non-Gaussianity of the likelihood, $z(\mathbf{x})|D_N$ is not Gaussian in general. However, it is still possible to show that (see e.g., Eqn 3.22 in [56])

$$\langle z(\mathbf{x}) \rangle_{p(z(\mathbf{x})|D_N)} = K(\mathbf{x}, X)K(X, X)^{-1}g(D_N), \quad (23)$$

where g is a function given by the expectation of the latent function given the training data. Consequently, as g is independent of \mathbf{x} , under boundedness assumption of $K(X, X)^{-1}g(D_N)$, the same approach considered in the proof of Theorem 1 following Eqn (17) holds also in this setting. \square

Corollary 2. Let $f(\mathbf{x}, \mathbf{w})$ be a BNN trained on a classification problem with data set $D_N = \{(\mathbf{x}_i, y_i) | i = 1, \dots, N, y_i \in \{0, 1\}\}$. Then, under the same assumptions of Theorem 1, for any $\mathbf{x} \in \mathcal{M}$ it holds that

$$\langle \nabla_{\mathbf{x}}^{\perp} f(\mathbf{x}) \rangle_{p(f(\mathbf{x}, \mathbf{w})|D_N)} \rightarrow 0.$$

Proof. The proof is analogous to that of Corollary 1 by noticing that in the infinitely-width limit (trained) BNNs converge to GPs also in the classification setting [57]. \square

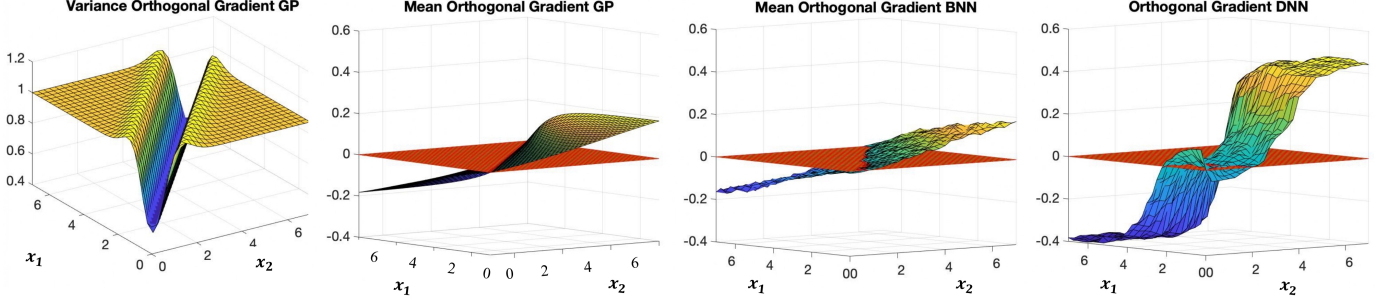


Fig. 1. We train a NN with ReLU activation functions and one hidden layer with 1024 hidden neurons. We consider a regression problem with data manifold given by the line $x_1 = x_2$ and data generated by function $\frac{2x_1^2}{10} - x_1$. We plot the mean and variance of the scalar projection of the gradient in a direction orthogonal to the data manifold for a GP with kernel corresponding to that of a BNN with ReLU activation functions and 1 hidden layer and compare it to the mean of the same quantity for a BNN trained with HMC and a NN with stochastic gradient descent. All NNs achieve accuracy $> 99\%$. Plane $z = 0$ is plotted in red.

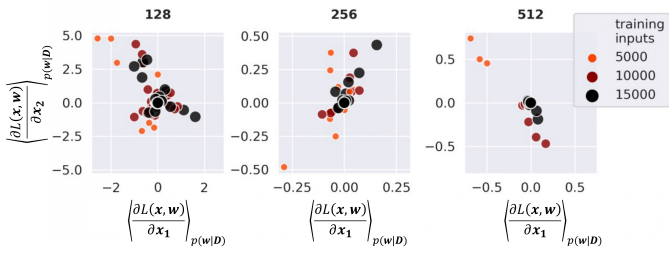


Fig. 2. We plot the two components of the expected loss gradient for BNNs trained on 100 two-dimensional test points from the Half Moons dataset [60]. We used a collection of HMC BNNs, by varying the number of hidden neurons (a different number in each subplot) and training points (different color and size of dots). Each dot represents a different NN. Only models with test accuracy greater than 80% are plotted.

TABLE I
HYPERPARAMETERS FOR TRAINING BNNs FOR FIGURE 2

Half moons grid search

Posterior samples	250
HMC warmup samples	100, 200, 500
Training inputs	5000, 10000, 15000
Hidden size	128, 256, 512
Nonlinear activation	Leaky ReLU
Architecture	2 fully connected layers

V. CONSEQUENCES AND LIMITATIONS OF OUR RESULTS

The results in the previous section have the natural consequence of protecting BNNs against gradient-based attacks, due to the vanishing average of the expectation of the gradients in the limit. Its proof also sheds light on a number of observations made in recent years. Before moving on to empirically validating the theorem in the finite-width case, it is worth reflecting on some of its implications and limitations:

- Theorem 1 holds in a specific thermodynamic limit, however we expect the averaging effect of BNN gradients to still provide considerable protection in conditions where the network architecture leads to high accuracy and strong expressivity. An empirical confirmation of this result is shown in Figure 2, where we examine the impact of the assumptions made in Theorem 1: by exploiting a setting in

which we have access to the data-generating distribution, the half-moons dataset [60] (details on training hyperparameters used can be found in Table I). We show that the magnitude of the expectation of each component of the gradient generally shrinks as we increase the number of network’s parameters and the number of training points. Notice that the trend is non-trivial as there is of course an interaction between the number of neurons per layer and the number of training points required to obtain an accurate posterior estimation (e.g., for 5000 training inputs when jumping from 256 to 512 neurons).

- Our results holds when the ensemble is drawn from the true posterior; nevertheless cheaper approximate Bayesian inference methods which retain ensemble predictions such as VI may still in practice provide good protection.
- Theorem 1 and 2 are stated for GPs. Consequently, these theorems not only provides theoretical backing to recent empirical observations of the adversarial robustness of GPs [61, 62, 63], but also generalizes to all processes that converge to GPs thanks to the Central Limit Theorem.
- While the Bayesian posterior ensemble may not be the only randomization to provide protection, it is clear that some simpler randomizations such as bootstrap will be ineffective, as noted empirically by [12]. This is because bootstrap resampling introduces variability along the data manifold, rather than in orthogonal directions. In this sense, bootstrap clearly cannot be considered a Bayesian approximation, especially when the data distribution has zero measure support w.r.t. the ambient space. Similarly, we do not expect gradient smoothing approaches to be successful [64], since the type of smoothing performed by Bayesian inference is specifically informed by the geometry of the data manifold.
- Our results only guarantees protection against gradient-based adversarial attacks. As a consequence, it is not clear if the robustness properties of BNNs also extend to non-gradient based attacks. Empirical results in Section VI-D also suggest that the vanishing gradient properties of BNNs may provide an increased robustness against specific gradient-free attacks.

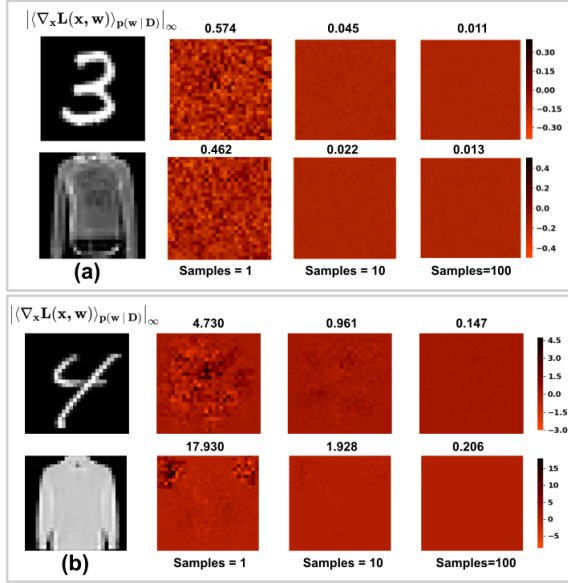


Fig. 3. We plot the infinite norm of the expected loss gradients for two BNNs trained on MNIST (Figure 3a) and Fashion MNIST (Figure 3b) for some example images and for different number of samples from the posterior predictive distribution. For training the BNN on MNIST we employed HMC, while VI is employed for Fashion MNIST. To the right of the images, we plot a heat map of gradient values. In all cases we observe that the expected loss gradient tends to decrease when increasing the number of samples.

VI. EMPIRICAL RESULTS

In this section we empirically investigate our theoretical findings on different BNNs. We train a variety of BNNs on the MNIST and Fashion MNIST [65] datasets (using their standard 60k/10k train-test split), and evaluate their posterior distributions using HMC and VI approximate inference methods. In Section VI-A, we experimentally verify the validity of the zero-averaging property of gradients implied by the theoretical results discussed in Section IV, and discuss its implications on the behaviours of FGSM and PGD attacks on BNNs in Section VI-B. In Section VI-C we analyse the relationship between robustness and accuracy on thousands of different NN architectures, comparing the results obtained by Bayesian and by deterministic training. Further, in Section VI-D we investigate the robustness of BNNs on a gradient-free adversarial attack [64].

A. Evaluation of the Gradient of the Loss for BNNs

We investigate the vanishing behavior of input gradients - established for the BNN classification case by Corollary 2 for the limit regime - in the finite, practical settings, that is with a finite-width BNN. Specifically, for each inference method we perform hyperparameter tuning and select the architecture achieving the highest test accuracy: we train a two hidden layers BNN (with 1024 neurons per layer) with HMC and a three hidden layers BNN (512 neurons per layer) with VI. These achieve approximately 95% test accuracy on MNIST and 89% on Fashion MNIST when trained with HMC; as well as 95% and 92%, respectively, when trained with VI. Details

about the hyperparameters used for training can be found in Tables II and III.

TABLE II
HYPERPARAMETERS FOR TRAINING BNNs USING HMC FOR FIGURES 3 AND 4.

Training hyperparameters for HMC

Dataset	MNIST	Fashion MNIST
Training inputs	60k	60k
Hidden size	1024	1024
Nonlinear activation	ReLU	ReLU
Architecture	Fully Connected	Fully Connected
Posterior Samples	500	500
Numerical Integrator	0.002	0.001
Stepsize		
Number of steps for Numerical Integrator	10	10

TABLE III
HYPERPARAMETERS FOR TRAINING BNNs USING VI FOR FIGURES 3 AND 4.

Training hyperparameters for VI

Dataset	MNIST	Fashion MNIST
Training inputs	60k	60k
Hidden size	512	1024
Nonlinear activation	Leaky ReLU	Leaky ReLU
Architecture	Convolutional	Convolutional
Training epochs	5	10
Learning rate	0.01	0.001

Figure 3 depicts anecdotal evidence on the behaviour of the component-wise expectation of the loss gradient as more samples from the posterior distribution are incorporated into the BNN predictive distribution. Similarly to how in Figure 2 for the half moons dataset we observe that the gradient of the loss goes to zero when increasing the number of training points and of parameters, here we have that, as the number of samples taken from the posterior distribution of w increases, all the components of the gradient approach zero. Notice that the gradients of the individual NNs (that is those with just one sampled weight vector), are markedly non-zero.

This is confirmed in Figure 4, where we provide a systematic analysis of the aggregated gradient convergence properties on 1k test images for MNIST and Fashion MNIST. Each dot shown in the plots represents a component of the expected loss gradient from each one of the images, for a total of 784k points used to visually approximate the empirical distribution of the component-wise expected loss gradient. For both HMC and VI the magnitude of the gradient components drops as the number of samples increases, and tends to stabilize around zero already with 100 samples drawn from the posterior distribution, suggesting that the limit conditions laid down in Corollary 2 are approximately met by the BNNs analysed here. Notice that the gradients computed on HMC trained networks drops more quickly and towards a smaller value compared to VI trained networks. This is in accordance to what is discussed in Section V, as VI introduces additional approximations in the Bayesian posterior computation.

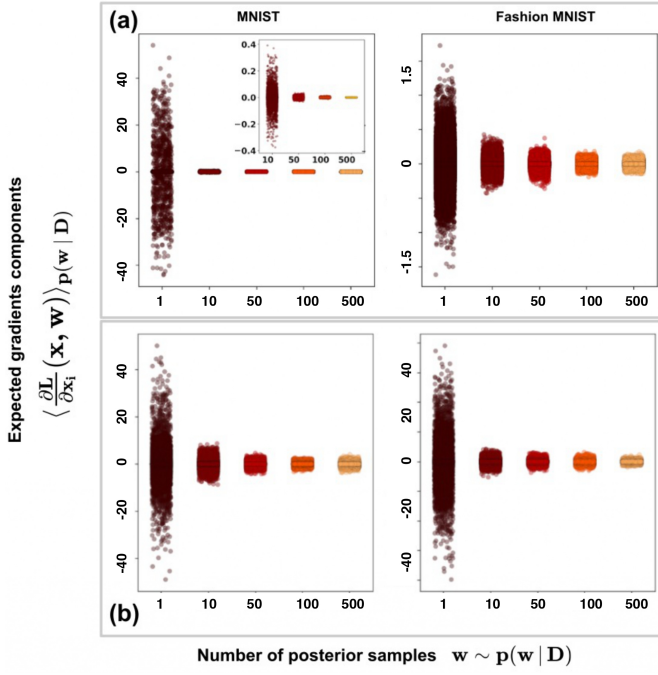


Fig. 4. The components of the expected loss gradients approach zero as the number of samples from the posterior distribution increases. For each number of samples, the figure shows 784 gradient components for 1k different test images, from both the MNIST and Fashion MNIST datasets. The gradients are computed on HMC (subfigure (a)) and VI (subfigure (b)) trained BNNs.

TABLE IV
ADVERSARIAL ROBUSTNESS OF BNNs TRAINED WITH HMC AND VI WITH
RESPECT TO FGSM, PGD AND CW.

Dataset/Method	Acc.	FGSM	PGD	CW
MNIST/SGD	0.984	0.376	0.334	0.358
MNIST/VI	0.974	0.623	0.508	0.512
MNIST/HMC	0.914	0.876	0.864	0.859
Fashion/SGD	0.891	0.510	0.410	0.432
Fashion/VI	0.862	0.622	0.581	0.588
Fashion/HMC	0.828	0.661	0.639	0.650

B. Gradient-Based Attacks for BNNs

The fact that gradient cancellation occurs in the limit does not directly imply that BNNs' predictions are robust to gradient-based attacks in the finite case. For example, FGSM attacks [2] are crafted such that the direction of the manipulation is given only by the sign of the expectation of the loss gradient and not by its magnitude. Thus, even if the entries of the expectation drop to an infinitesimal magnitude but maintain a meaningful sign, then FGSM could potentially produce effective attacks. In order to test the implications of vanishing gradients on the robustness of the posterior predictive distribution against gradient-based attacks, we compare the behaviour of FGSM, PGD⁹ [5] and CW [66] attacks, arguably the most commonly employed gradient-based attacks.

In particular, in Table IV we evaluate a single hidden-layer neural network architecture with 512 hidden neurons trained on MNIST and Fashion MNIST using HMC, VI, and SGD.

⁹With 15 iterations and 1 restart.

We then attack it using attack strength $\epsilon = 0.1$ for MNIST and $\epsilon = 0.05$ for FashionMNIST. For each image, we compute the expected gradient using 50 posterior samples. Details on the hyper-parameters used in each setting can be found in Tables V–VII (entries marked with a *). We observe that BNNs are generally more robust against each of the gradient-based attacks. Interestingly, we also notice that for BNNs, FGSM performs comparably to PGD and CW attacks with little increase in attack success rate when using stronger attacks. Furthermore, we should also note that for FashionMNIST, the attacks are more successful than in the MNIST case. As FashionMNIST poses a more complicated classification problem than MNIST, the BNNs obtain less accuracy in the former. In agreement with the discussion in Section V, this implies higher loss and that the conditions set up in the main theorems and corollaries are less approximately met.

TABLE V
HYPERPARAMETERS FOR TRAINING BNNs WITH HMC IN FIGURE 5. *
INDICATES THE PARAMETERS USED IN TABLE IV.

HMC MNIST/Fashion MNIST grid search

Posterior samples	{250*, 500, 750}
Numerical Integrator Stepsize	{0.025*, 0.01, 0.005, 0.001, 0.0001}
Numerical Integrator Steps	{10, 15, 20*}
Hidden size	{128, 256, 512*}
Nonlinear activation	{relu*, tanh, sigmoid}
Architecture	{1*, 2, 3} fully connected layers

TABLE VI
HYPERPARAMETERS FOR TRAINING BNNs WITH VI IN FIGURE 5. *
INDICATES THE PARAMETERS USED IN TABLE IV.

VI MNIST/Fashion MNIST grid search

Learning Rate	{0.001*}
Minibatch Size	{128*, 256, 512, 1024}
Hidden size	{64, 128, 256, 512*, 1024}
Nonlinear activation	{relu*, tanh, sigmoid}
Architecture	{1*, 2, 3} fully connected layers
Training epochs	{3, 5, 7, 9, 12, 15*} epochs

TABLE VII
HYPERPARAMETERS FOR TRAINING NNS WITH SGD IN FIGURE 5. *
INDICATES THE PARAMETERS USED IN TABLE IV.

SGD MNIST/Fashion MNIST grid search

Learning Rate	{0.001, 0.005, 0.01, 0.05*}
Hidden size	{64, 128, 256, 512*}
Nonlinear activation	{relu*, tanh, sigmoid}
Architecture	{1*, 2, 3, 4, 5} fully connected layers
Training epochs	{5, 10, 15, 20*, 25} epochs

C. Robustness Accuracy Analysis in Deterministic and Bayesian Neural Networks

In Section V, we noticed that, as proxy of the loss and of convergence, high accuracy might be related to high robustness to gradient-based attacks for BNNs. Notice, that this would run counter to what has been observed for deterministic NNs trained with SGD [67].

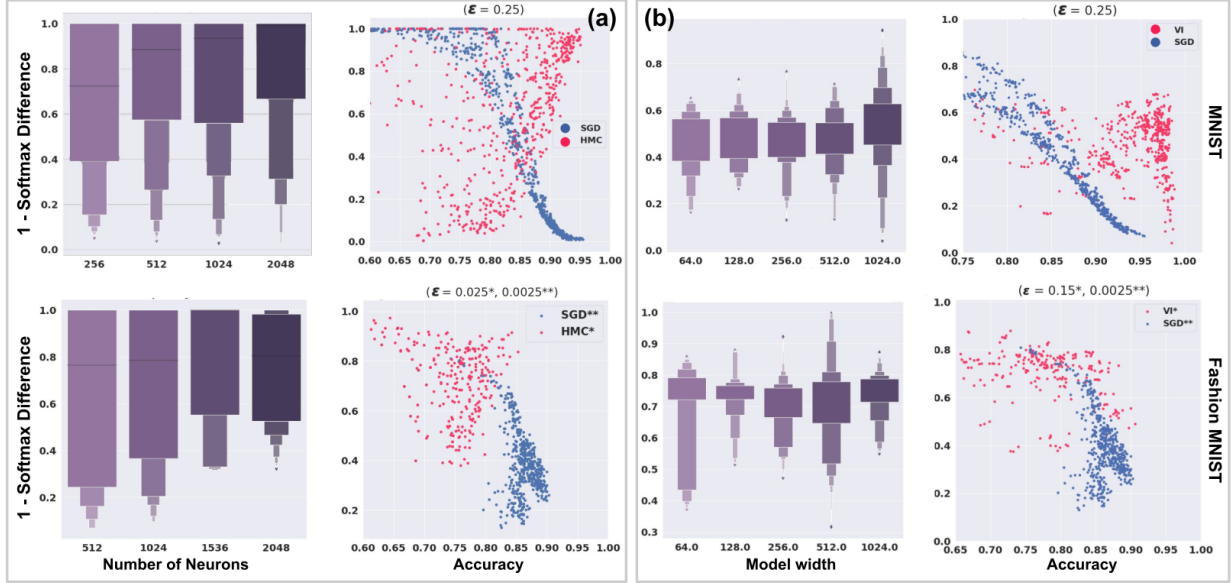


Fig. 5. Robustness-Accuracy trade-off on MNIST (first row) and Fashion MNIST (second row) for BNNs trained with HMC (a), VI (b) and SGD (blue dots). While a trade-off between accuracy and robustness occur for deterministic NNs, experiments on HMC show a positive correlation between accuracy and robustness. The boxplots show the correlation between model capacity and robustness. Different attack strength (ϵ) are used for the three methods accordingly to their average robustness.

In this section, we look at an array of more than 1000 BNNs with different hyperparameters trained with HMC and VI on MNIST and Fashion MNIST (details on training and architecture hyper-parameters explored can be found in Tables V–VII). We experimentally evaluate their accuracy/robustness trade-off on FGSM attacks as compared to that of the same neural network architectures trained via standard (i.e., non-Bayesian) SGD based methods. For the robustness evaluation we consider the average difference in the softmax prediction between the original test points and the crafted adversarial input, as this provides a quantitative and smooth measure of adversarial robustness that is closely related with misclassification ratios [68]. That is, for a collection of N test point, we compute

$$\frac{1}{N} \sum_{j=1}^N \left| \langle f(\mathbf{x}_j, \mathbf{w}) \rangle_{p(\mathbf{w}|D)} - \langle f(\tilde{\mathbf{x}}_j, \mathbf{w}) \rangle_{p(\mathbf{w}|D)} \right|_\infty. \quad (24)$$

The results of the analysis are plotted in Figure 5. Each dot in the scatter plots represents the results obtained for each specific network architecture trained with SGD (blue dots), HMC (pink dots in plots (a)) and VI (pink dots in plots (b)). As already reported in the literature [67] we observe a marked trade-off between accuracy and robustness (i.e., 1 - softmax difference) for high-performing deterministic networks. Interestingly, this trend is reversed for BNNs trained with HMC (plots (a) in Figure 5) where we find that as networks become more accurate, they additionally become more robust to FGSM attacks as well. We further examine this trend in the boxplots that represent the effect that the network width has on the robustness of the resulting posterior. We find the existence of an increasing trend in robustness as the number of neurons in the network is increased. This is in line with our theoretical findings, i.e., as the BNN approaches the infinite width limit, the conditions for

Corollary 2 are approximately met and the network is protected against gradient-based attacks.

On the other hand, the trade-off behaviours are less obvious for the BNNs trained with VI and on Fashion-MNIST. In particular, in plot (b) of Figure 5 we find that, similarly to the deterministic case, also for BNNs trained with VI, robustness seems to have a negative correlation with accuracy, albeit less marked than for SGD. Furthermore, similarly than for HMC, we also observe that for VI the robustness of the BNNs tend to increase with the width of the network. However, the trend is less clear compared to the HMC case. This can be linked to the fact that VI is known to often under-approximate uncertainty [56], which may lead to posterior with excessively small variance, thus behaving similarly to a deterministic NN. We should also emphasize that experimental results in this paper have been performed with Bayes by backprop [46]. However, approximate Bayesian inference techniques for deep learning is an active area of research, including recent developments, e.g., SWAG [69] or Noisy Adam [70], such developments could, in principle, lead to a behaviour closer to that exhibited by HMC.

D. Gradient-Free Adversarial Attacks

In this section, we empirically evaluate the most accurate BNN posteriors on MNIST and Fashion MNIST from Figure 5 against gradient-free adversarial attacks. Specifically, we consider ZOO [71], a gradient-free adversarial attack based on a finite-difference approximation of the gradient of the loss obtained by querying the neural network (in the BNN case the attacker queries the posterior distribution). In particular, we selected ZOO because it has been shown to be effective even when tested on networks that purposefully obfuscate their gradients or have vanishing gradients [64]. In Figure 6 we observe that similarly to gradient-based methods, ZOO is

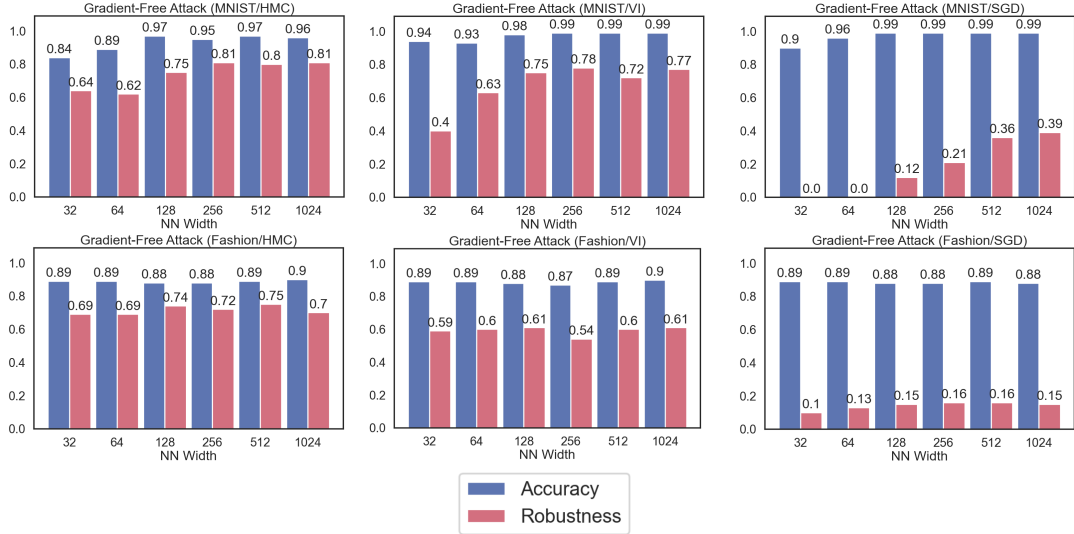


Fig. 6. Gradient-free adversarial attacks on BNNs display similar behavior to gradient-based attacks. We evaluate the more accurate networks from Figure 5 with gradient-free attacks on MNIST (first row) and Fashion MNIST (second row) for BNNs trained with HMC (left column), VI (center column), and SGD (right column). We use the same attack parameters as in the Figure 5, but use ZOO as an attack method.

substantially less effective on BNNs compared to deterministic NNs in all cases, with BNNs again achieving both high accuracy and high robustness simultaneously. Furthermore, once again HMC is more robust to the attack than VI, which is in turn substantially more robust than deterministic NNs. This suggests how, similarly to what observed in the previous subsections, a more accurate posterior distribution may lead to a more robust model also to gradient-free adversarial attacks.

VII. CONCLUSIONS

The quest for robust, data-driven models is an essential component towards the construction of AI-based technologies. In this respect, we believe that the fact that Bayesian ensembles of NNs can provide additional robustness against a broad class of adversarial attacks will be of great relevance. While promising, this result comes with some significant limitations. First, our theoretical results hold in a thermodynamic limit, which is never realised in practice. More worryingly, we currently have no rigorous diagnostics to understand how near we are to the limit case, and can only reason about this empirically. Secondly, and perhaps more importantly, performing Bayesian inference in large non-linear models is extremely challenging. In fact, while in our experiments cheaper approximations, such as VI, also enjoyed a degree of adversarial robustness, albeit reduced, there are no guarantees that this will hold in general. To this end, we hope that this result will spark renewed interest in the pursuit of efficient Bayesian inference algorithms, which have the potential to lead to learning models that are intrinsically accurate and robust.

REFERENCES

- [1] C. Szegedy, W. Zaremba, I. Sutskever, J. Bruna, D. Erhan, I. Goodfellow, and R. Fergus, “Intriguing properties of neural networks,” *arXiv preprint arXiv:1312.6199*, 2013.
- [2] I. J. Goodfellow, J. Shlens, and C. Szegedy, “Explaining and harnessing adversarial examples,” *arXiv preprint arXiv:1412.6572*, 2014.
- [3] J. Zhang and C. Li, “Adversarial examples: Opportunities and challenges,” *IEEE transactions on neural networks and learning systems*, vol. 31, no. 7, pp. 2578–2593, 2019.
- [4] B. Biggio and F. Roli, “Wild patterns: Ten years after the rise of adversarial machine learning,” *Pattern Recognition*, vol. 84, pp. 317–331, 2018.
- [5] A. Madry, A. Makelov, L. Schmidt, D. Tsipras, and A. Vladu, “Towards deep learning models resistant to adversarial attacks,” 2017.
- [6] R. M. Neal, *Bayesian learning for neural networks*. Springer Science & Business Media, 2012, vol. 118.
- [7] X. Jia, H. Gu, Y. Liu, J. Yang, X. Wang, W. Pan, Y. Zhang, S. Cotofana, and W. Zhao, “An energy-efficient bayesian neural network implementation using stochastic computing method,” *IEEE Transactions on Neural Networks and Learning Systems*, 2023.
- [8] H. Li, P. Barnaghi, S. Enshaeifar, and F. Ganz, “Continual learning using bayesian neural networks,” *IEEE transactions on neural networks and learning systems*, vol. 32, no. 9, pp. 4243–4252, 2020.
- [9] J.-T. Chien and Y.-C. Ku, “Bayesian recurrent neural network for language modeling,” *IEEE transactions on neural networks and learning systems*, vol. 27, no. 2, pp. 361–374, 2015.
- [10] R. Feinman, R. R. Curtin, S. Shintre, and A. B. Gardner, “Detecting adversarial samples from artifacts,” *arXiv preprint arXiv:1703.00410*, 2017.
- [11] M. Wicker, L. Laurenti, A. Patane, Z. Chen, Z. Zhang, and M. Kwiatkowska, “Bayesian inference with certifiable adversarial robustness,” in *International Conference on Artificial Intelligence and Statistics*. PMLR, 2021, pp. 2431–2439.
- [12] A. Bekasov and I. Murray, “Bayesian adversarial spheres:

Bayesian inference and adversarial examples in a noiseless setting,” *arXiv preprint arXiv:1811.12335*, 2018.

[13] X. Liu, Y. Li, C. Wu, and C.-J. Hsieh, “Adv-bnn: Improved adversarial defense through robust bayesian neural network,” *arXiv preprint arXiv:1810.01279*, 2018.

[14] M. Yuan, M. Wicker, and L. Laurenti, “Gradient-free adversarial attacks for bayesian neural networks,” *arXiv preprint arXiv:2012.12640*, 2020.

[15] J. M. Lee, “Smooth manifolds,” in *Introduction to smooth manifolds*. Springer, 2013, pp. 1–31.

[16] G. Carbone, M. Wicker, L. Laurenti, A. Patane, L. Bortolussi, and G. Sanguinetti, “Robustness of bayesian neural networks to gradient-based attacks,” *Advances in Neural Information Processing Systems*, vol. 33, pp. 15 602–15 613, 2020.

[17] C. Liu, M. Salzmann, and S. Süsstrunk, “Training provably robust models by polyhedral envelope regularization,” *IEEE Transactions on Neural Networks and Learning Systems*, 2021.

[18] R. R. Wiyatno, A. Xu, O. Dia, and A. De Berker, “Adversarial examples in modern machine learning: A review,” *arXiv preprint arXiv:1911.05268*, 2019.

[19] X. Yuan, P. He, Q. Zhu, and X. Li, “Adversarial examples: Attacks and defenses for deep learning,” *IEEE transactions on neural networks and learning systems*, vol. 30, no. 9, pp. 2805–2824, 2019.

[20] A.-J. Gallego, J. Calvo-Zaragoza, and R. B. Fisher, “Incremental unsupervised domain-adversarial training of neural networks,” *IEEE Transactions on Neural Networks and Learning Systems*, vol. 32, no. 11, pp. 4864–4878, 2020.

[21] P. Panda, “Quanos: adversarial noise sensitivity driven hybrid quantization of neural networks,” in *Proceedings of the ACM/IEEE International Symposium on Low Power Electronics and Design*, 2020, pp. 187–192.

[22] A. Ilyas, S. Santurkar, D. Tsipras, L. Engstrom, B. Tran, and A. Madry, “Adversarial examples are not bugs, they are features,” *Advances in neural information processing systems*, vol. 32, 2019.

[23] J. Lin, C. Gan, and S. Han, “Defensive quantization: When efficiency meets robustness,” in *International Conference on Learning Representations*. International Conference on Learning Representations, ICLR, 2019.

[24] D. Tsipras, S. Santurkar, L. Engstrom, A. Turner, and A. Madry, “Robustness may be at odds with accuracy,” *arXiv preprint arXiv:1805.12152*, 2018.

[25] Y. Pang, S. Cheng, J. Hu, and Y. Liu, “Evaluating the robustness of bayesian neural networks against different types of attacks,” *arXiv preprint arXiv:2106.09223*, 2021.

[26] L. Smith and Y. Gal, “Understanding measures of uncertainty for adversarial example detection,” *arXiv preprint arXiv:1803.08533*, 2018.

[27] A. Uchendu, D. Campoy, C. Menart, and A. Hildenbrandt, “Robustness of bayesian neural networks to white-box adversarial attacks,” in *2021 IEEE Fourth International Conference on Artificial Intelligence and Knowledge Engineering (AIKE)*. IEEE, 2021, pp. 72–80.

[28] R. Michelmore, M. Wicker, L. Laurenti, L. Cardelli, Y. Gal, and M. Kwiatkowska, “Uncertainty quantification with statistical guarantees in end-to-end autonomous driving control,” in *2020 IEEE International Conference on Robotics and Automation (ICRA)*. IEEE, 2020, pp. 7344–7350.

[29] Y. Gal and L. Smith, “Sufficient conditions for idealised models to have no adversarial examples: a theoretical and empirical study with bayesian neural networks,” *arXiv preprint arXiv:1806.00667*, 2018.

[30] A. Rawat, M. Wistuba, and M.-I. Nicolae, “Adversarial phenomenon in the eyes of bayesian deep learning,” *arXiv preprint arXiv:1711.08244*, 2017.

[31] N. Carlini and D. Wagner, “Adversarial examples are not easily detected: Bypassing ten detection methods,” in *Proceedings of the 10th ACM Workshop on Artificial Intelligence and Security*, 2017, pp. 3–14.

[32] K. Grosse, D. Pfaff, M. T. Smith, and M. Backes, “The limitations of model uncertainty in adversarial settings,” *arXiv preprint arXiv:1812.02606*, 2018.

[33] M. Wicker, L. Laurenti, A. Patane, and M. Kwiatkowska, “Probabilistic safety for bayesian neural networks,” in *Conference on Uncertainty in Artificial Intelligence*. PMLR, 2020, pp. 1198–1207.

[34] L. Berrada, S. Dathathri, R. Stanforth, R. Bunel, J. Uesato, S. Gowal, M. P. Kumar *et al.*, “Verifying probabilistic specifications with functional lagrangians,” *arXiv preprint arXiv:2102.09479*, 2021.

[35] J. Zhang, Y. Hua, Z. Xue, T. Song, C. Zheng, R. Ma, and H. Guan, “Robust bayesian neural networks by spectral expectation bound regularization,” in *Proceedings of the IEEE/CVF Conference on Computer Vision and Pattern Recognition*, 2021, pp. 3815–3824.

[36] N. Ye and Z. Zhu, “Bayesian adversarial learning,” in *Proceedings of the 32nd International Conference on Neural Information Processing Systems*. Curran Associates Inc., 2018, pp. 6892–6901.

[37] C. M. Bishop *et al.*, *Neural networks for pattern recognition*. Oxford university press, 1995.

[38] G. Cybenko, “Approximation by superpositions of a sigmoidal function,” *Mathematics of control, signals and systems*, vol. 2, no. 4, pp. 303–314, 1989.

[39] K. Hornik, “Approximation capabilities of multilayer feedforward networks,” *Neural networks*, vol. 4, no. 2, pp. 251–257, 1991.

[40] A. G. d. G. Matthews, M. Rowland, J. Hron, R. E. Turner, and Z. Ghahramani, “Gaussian process behaviour in wide deep neural networks,” *arXiv preprint arXiv:1804.11271*, 2018.

[41] G. Ongie, R. Willett, D. Soudry, and N. Srebro, “A function space view of bounded norm infinite width relu nets: The multivariate case,” in *International Conference on Learning Representations*, 2020.

[42] G. M. Rotskoff and E. Vanden-Eijnden, “Neural networks as interacting particle systems: Asymptotic convexity of the loss landscape and universal scaling of the approximation error,” *arXiv preprint arXiv:1805.00915*, 2018.

[43] D. Barber, *Bayesian reasoning and machine learning*. Cambridge University Press, 2012.

[44] C. M. Bishop, *Pattern Recognition and Machine Learning (Information Science and Statistics)*. Berlin, Heidelberg: Springer-Verlag, 2006.

[45] R. M. Neal *et al.*, “Mcmc using hamiltonian dynamics,” *Handbook of markov chain monte carlo*, vol. 2, no. 11, p. 2, 2011.

[46] C. Blundell, J. Cornebise, K. Kavukcuoglu, and D. Wierstra, “Weight uncertainty in neural networks,” *arXiv preprint arXiv:1505.05424*, 2015.

[47] R. J. Adler, *The geometry of random fields*. SIAM, 2010.

[48] P. Billingsley, *Convergence of probability measures*. John Wiley & Sons, 2013.

[49] J. Lee, Y. Bahri, R. Novak, S. S. Schoenholz, J. Pennington, and J. Sohl-Dickstein, “Deep neural networks as gaussian processes,” *arXiv preprint arXiv:1711.00165*, 2017.

[50] A. Garriga-Alonso, C. E. Rasmussen, and L. Aitchison, “Deep convolutional networks as shallow gaussian processes,” *arXiv preprint arXiv:1808.05587*, 2018.

[51] A. Fawzi, H. Fawzi, and O. Fawzi, “Adversarial vulnerability for any classifier,” in *Advances in Neural Information Processing Systems*, 2018, pp. 1178–1187.

[52] M. Khouri and D. Hadfield-Menell, “On the geometry of adversarial examples,” *arXiv preprint arXiv:1811.00525*, 2018.

[53] S. Goldt, M. Mézard, F. Krzakala, and L. Zdeborová, “Modelling the influence of data structure on learning in neural networks,” *arXiv preprint arXiv:1909.11500*, 2019.

[54] C. Anders, P. Pasliev, A.-K. Dombrowski, K.-R. Müller, and P. Kessel, “Fairwashing explanations with off-manifold detergent,” in *International Conference on Machine Learning*. PMLR, 2020, pp. 314–323.

[55] H. Liu, Y.-S. Ong, X. Shen, and J. Cai, “When gaussian process meets big data: A review of scalable gps,” *IEEE transactions on neural networks and learning systems*, vol. 31, no. 11, pp. 4405–4423, 2020.

[56] C. E. Rasmussen *et al.*, *Gaussian processes for machine learning*. Springer, vol. 1.

[57] J. Hron, Y. Bahri, R. Novak, J. Pennington, and J. Sohl-Dickstein, “Exact posterior distributions of wide bayesian neural networks,” *arXiv preprint arXiv:2006.10541*, 2020.

[58] R. Novak, L. Xiao, Y. Bahri, J. Lee, G. Yang, J. Hron, D. A. Abolafia, J. Pennington, and J. Sohl-dickstein, “Bayesian deep convolutional networks with many channels are gaussian processes,” in *International Conference on Learning Representations*, 2018.

[59] B.-H. Tran, S. Rossi, D. Milios, and M. Filippone, “All you need is a good functional prior for bayesian deep learning,” *Journal of Machine Learning Research*, vol. 23, no. 74, pp. 1–56, 2022.

[60] A. Rozza, M. Manzo, and A. Petrosino, “A novel graph-based fisher kernel method for semi-supervised learning,” in *2014 22nd International Conference on Pattern Recognition*. IEEE, 2014, pp. 3786–3791.

[61] L. Cardelli, M. Kwiatkowska, L. Laurenti, and A. Patane, “Robustness guarantees for bayesian inference with gaussian processes,” in *Proceedings of the AAAI Conference on Artificial Intelligence*, vol. 33, 2019, pp. 7759–7768.

[62] K. Grosse, M. T. Smith, and M. Backes, “Killing four birds with one gaussian process: the relation between different test-time attacks,” in *2020 25th International Conference on Pattern Recognition (ICPR)*. IEEE, 2021, pp. 4696–4703.

[63] A. Patane, A. Blaas, L. Laurenti, L. Cardelli, S. Roberts, and M. Kwiatkowska, “Adversarial robustness guarantees for gaussian processes,” *Journal of Machine Learning Research*, vol. 23, pp. 1–55, 2022.

[64] A. Athalye, N. Carlini, and D. Wagner, “Obfuscated gradients give a false sense of security: Circumventing defenses to adversarial examples,” *arXiv preprint arXiv:1802.00420*, 2018.

[65] H. Xiao, K. Rasul, and R. Vollgraf, “Fashion-mnist: a novel image dataset for benchmarking machine learning algorithms,” *arXiv preprint arXiv:1708.07747*, 2017.

[66] N. Carlini and D. Wagner, “Towards evaluating the robustness of neural networks,” 2016.

[67] D. Su, H. Zhang, H. Chen, J. Yi, P.-Y. Chen, and Y. Gao, “Is robustness the cost of accuracy?—a comprehensive study on the robustness of 18 deep image classification models,” in *Proceedings of the European Conference on Computer Vision (ECCV)*, 2018, pp. 631–648.

[68] L. Cardelli, M. Kwiatkowska, L. Laurenti, N. Paoletti, A. Patane, and M. Wicker, “Statistical guarantees for the robustness of bayesian neural networks,” in *IJCAI*, 2019.

[69] W. J. Maddox, P. Izmailov, T. Garipov, D. P. Vetrov, and A. G. Wilson, “A simple baseline for bayesian uncertainty in deep learning,” *Advances in neural information processing systems*, vol. 32, 2019.

[70] G. Zhang, S. Sun, D. Duvenaud, and R. Grosse, “Noisy natural gradient as variational inference,” in *International conference on machine learning*. PMLR, 2018, pp. 5852–5861.

[71] P.-Y. Chen, H. Zhang, Y. Sharma, J. Yi, and C.-J. Hsieh, “Zoo: Zeroth order optimization based black-box attacks to deep neural networks without training substitute models,” in *Proceedings of the 10th ACM workshop on artificial intelligence and security*, 2017, pp. 15–26.